IJAAR PUBLISHING®

Engineering Research Journal | ISSN: 2782-8212
Vol. 3, Issue 12 (December, 2023) | www.ijaar.org/erj

EXPERIMENTAL INVESTIGATION OF THE PHOTOPHYSICAL PROPERTIES OF OPTIMIZED NANO-SILICA DERIVED FROM DIFFERENT WEIGHTS OF RICE HUSK

[1]A. J. KPELAI & [2]C. MBAKAAN

[1] Department of Electrical/ Electronic Engineering, Benue State Polytechnic, Ugbokolo.
[2] Department of Science Laboratory Technology, Physics/Electronic Section, Benue State Polytechnic, Ugbokolo.

Corresponding Author E-mail- celestinembakaan@gmail.com.

Abstract
The effect of the initial starting weight of rice husk (RH) on the photophysical properties of nano-silica (RHS) has been explored. The nano-silica was produced by pretreating RH with acids and subsequent thermal treatment. The analysis of surface morphology revealed that all the samples contained agglomerates of spherical nanosized particles, with larger particles produced from higher starting weights of rice husk. The optical properties of the RHS are due to more than one defect or center, including oxygen-deficiency centers (ODCs), non-bridging oxygen holecenters (NBOHC), and carbon impurities. The emission color of the RHS samples shifts from blue to near-white light as the weight of the starting RH increases due to an increase in the carbon residue left in the samples. This nano-silica is ideal for use in photonics and other engineering applications.

Keywords: Optimized nanosilica; Photophysical Properties; weights, Rice Husk; Morphology; Photoluminescence

09/12/2023
A. J. Kpelai & C. Mbakaan. (2023). Experimental Investigation of the Photophysical Properties of Optimized Nano-Silica Derived from Different Weights of Rice Husk. *Engineering Research Journal*, 3(12), 1-15.

1.0 Introduction

Rice husk is a significant biomass that has received attention for energy and engineering applications. It is cost-effective and boasts a high silica content that makes it suitable for various engineering purposes. Rice husk (RH) is a promising raw material for producing silica nanoparticles since it contains a substantial amount of silica (approximately 15-28 Wt %)[1,2]. By adjusting experimental conditions such as the chemical pretreatment method, calcination temperature, time, and environment during synthesis, silica nanoparticles can be produced from RH [1].

Nano-silica, also known as silica nanoparticles, has gained significant attention due to its stability, low toxicity, and versatility in being functionalized with different molecules and polymers. It finds widespread applications in energy and biomedical research and has been the subject of various studies including the studies conducted by Nobre et al., Bardosova et al., Zhang and Lin, and Rossi et al.[3–6]. Carbon-incorporated nano-silica is also gaining popularity for producing white phosphors, as evidenced inthe research conducted by Ishikawa et al., Chen, Liu et al., and Wang et al.[2,7–9].

Past research has relied on expensive and toxic chemicals such as alkoxysilanes and polysiloxanes to synthesize silica nanoparticles, as Green et al.[10] and Narisawa et al.[11]reported. However, the need for a safer, more environmentally friendly, and simpler method to produce chemically and thermally stable nano-silica has been highlighted by Bryant et al.[12].

Several researchers, including Chen [8], Ishikawa et al. [7], and Wang et al. [2], have successfully synthesized silica nanoparticles from rice husks by utilizing hydrochloric acid as a pretreatment agent, to produce phosphors. Further details on the purification of rice husks and the production of high-purity silica using phosphoric acid have been reported by Mbakaan et al. [13]. The effects of various factors, such as location, doping, and rice variety, on the photophysical properties of silica derived from rice husks have also been investigated[14]. While these studies have yielded impressive results, the impact of the initial quantity of rice husk on the properties of the resulting nano-silica has not been comprehensively explored. Chen [8] only examined the influence of the starting amount of RHs on the emission intensity, without a detailed investigation of the underlying mechanism or variations in structural, surface morphology, and optical, characteristics. Herein, our research aims to close this gap by creating nanosilica using varying starting amounts of rice husk (1-5g) and examining how the starting quantity affects the photophysical properties such as structure, morphology, chemical composition, and optical properties of the resulting nanosilica.

2.0 Materials and Methods

Husk of Osi (Nerica-I) rice variety (Oryza Sativa species)was collected from Wurukum rice milling station, Makurdi, Benue state, Nigeria. A mesh of size 75 microns and a pan were used to sieve the rice husk samples. The husks were boiled in HCl, washed, and dried in an oven at a temperature of 100 $^{\circ}$C. Dried HCl pretreated RHs of amounts 1g, 2g, 3g, 4g, and 5g were weighed using an electronic balance with an accuracy of 0.001. The samples were placed in crucibles and calcined at a temperature of 550 $^{\circ}$C for 6 hrs. The ramping rate was 10 $^{\circ}$C /min until the temperature reached 550 $^{\circ}$C. The samples were allowed to cool naturally overnight.

Nanotechnology tools, such as an X-ray Diffraction (XRD) machine for structural analysis, a Field Emission Scanning Electron Microscope (FESEM), and a Transmission Electron

Microscope (TEM) for surface morphology, were used to analyze the samples. Both SEM and TEM were equipped with energy-dispersive X-ray spectroscopy (EDX) to study chemical composition. Fourier Transform Infrared Spectroscopy (FTIR) was conducted with a Perkin-Elmer Ate-FTIR 100 spectrometer, and the BET Surface area analyzer model Micromeritics TRISTAR II 3020 was employed to determine the surface area. UV-Vis spectroscopy was performed at room temperature using a Perkin-Elmer Lambda 1050 UV/Vis/NIR spectrophotometer equipped with an integrating sphere, while Photoluminescence (PL) measurements were taken using a Hitachi F-7000 spectrophotometer.

3.0 Results and Discussion

3.1 Structural Analysis

Figure 1 depicts the X-ray diffraction (XRD) patterns of nano-silica (RHS) produced from varying amounts of RH (RHS-x RH where x= 1g, 5g). Each sample's XRD pattern displays a broad peak ranging from 15 to 30°, with a maximum at 2θ ~22.19°, indicating amorphous silica [15,16]. Besides, all the patterns exhibit a crystalline peak at approximately 2θ ~26.58°, assigned to miller indices (101), and belonging to the silica phase (COD card no. 96-710-3015). RHS-1g RH's XRD pattern also displays a peak at 2θ= 20.89, assigned to miller indices (100), matching the silica phase in COD card no. 96-710-3015. RHS-4g RH's XRD pattern shows minor peaks at 2θ= 39.46, 42.45, 59.97, and 68.21°, assigned to Miller indices (102), (200), (211), and (203), respectively, and matching the silica phase in COD card no. 96-710-3015. These findings confirm the synthesis of pure and amorphous silica from all the samples.

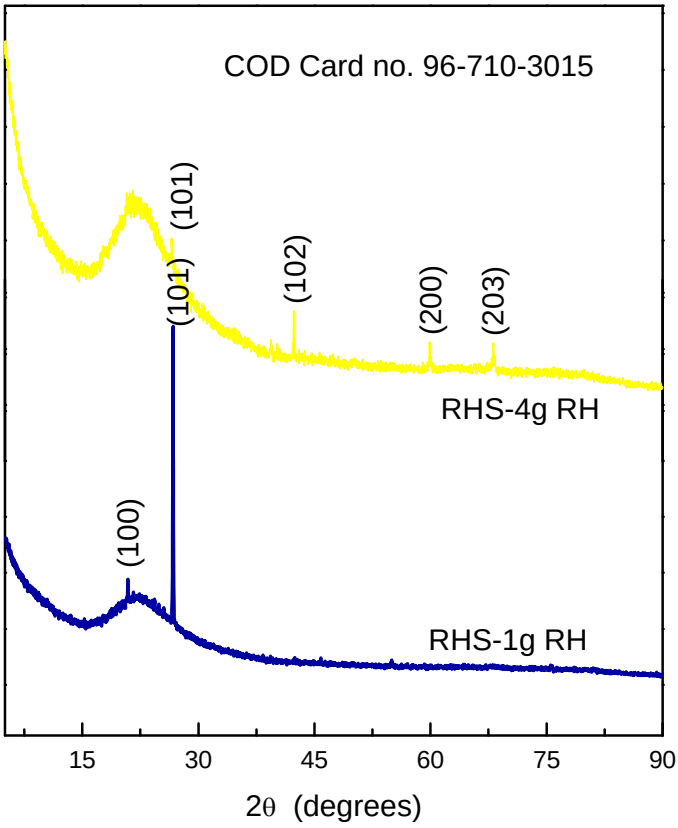


Fig 1. XRD patterns ofnano-silicaderived from varying starting amounts of RHs

3.2 Surface Morphology and Chemical Composition.

We conducted a thorough investigation to examine the surface morphology characteristics of nano-silica (RHS) extracted from RH of varying masses, specifically RHS-1g RH and RHS-4g RH. Our analysis was conducted by utilizing Field Emission Scanning Electron Microscopy (FESEM) and Transmission Electron Microscopy (TEM) techniques. Figures 2(a) and (b) display the FESEM micrographs of nano-silica (RHS) derived from RH of varying masses, namely RHS-1g RH and RHS-4g RH. The images reveal the formation of irregularly shaped agglomerates of nano-sized particles. Furthermore, Figures 2 (c) and (d) present the TEM micrographs of RHS from RH of different masses RHS-1g RH and RHS-4g respectively. The TEM micrographs showcase the formation of spherical-shaped particles that are also nano-sized. Upon analyzing the TEM micrographs, we discovered that the average particle sizes are roughly 45 nm and 49 nm for RHS-1g RH and RHS-4g respectively, as shown in Table 1. This result implies that larger particles can be created by using more starting rice husks, which is also supported by the XRD result. Furthermore, our surface morphology analysis using FESEM and TEM provided additional confirmation of the amorphous nature of the samples. In addition, the selected area electron diffraction (SAED) pattern shown in Figure 2 (e) validated the amorphous nature of the nano-silica, as indicated by the absence of concentric rings and the presence of a halo around the bright center spot. These observations suggest that the electrons are scattered randomly by the amorphous structure of the sample [17].

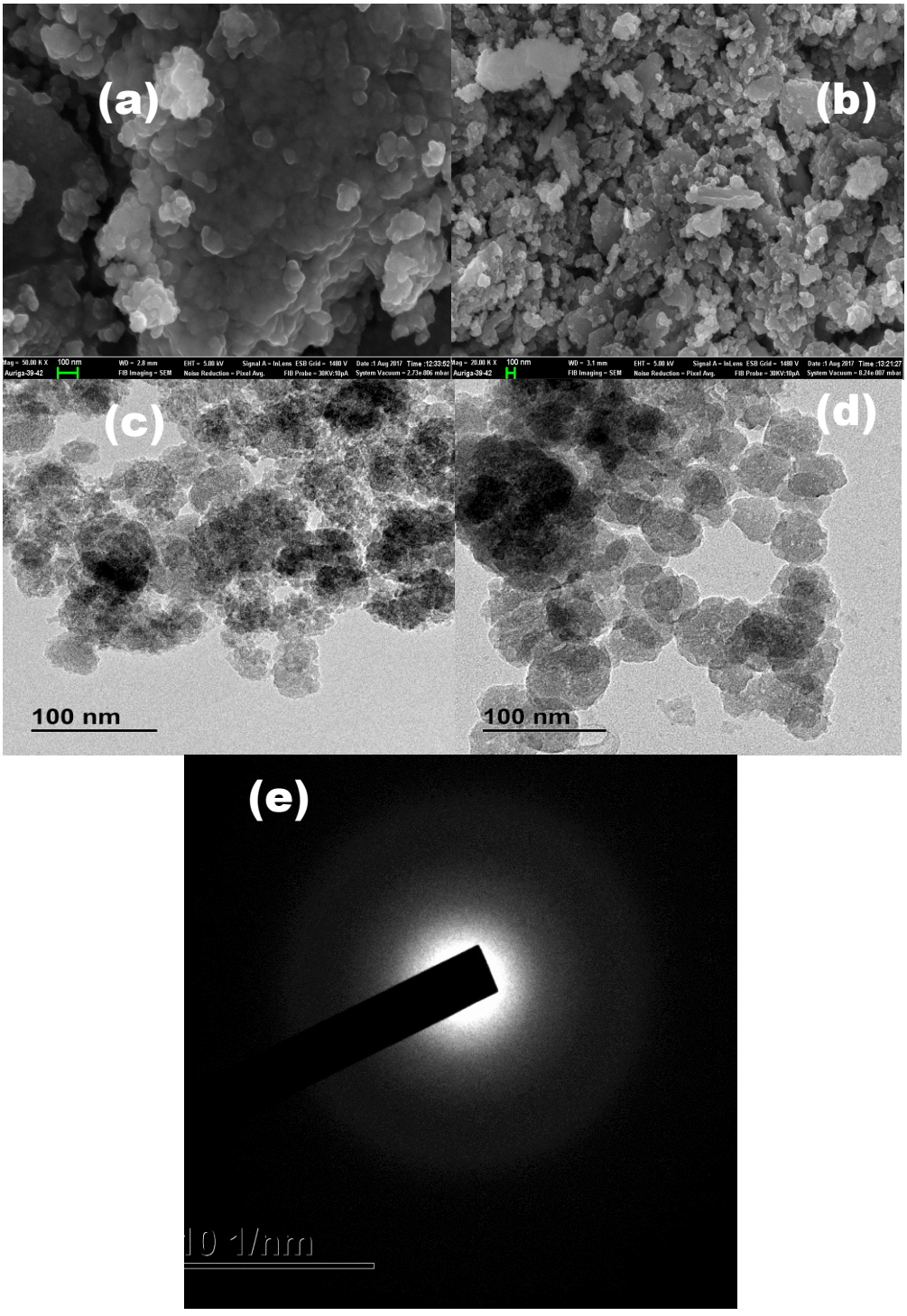


Fig 2. (a) SEM image of RHS-1g RH (b) SEM image of RHS-4g RH
(c) TEM image of RHS-1g RH (d) TEM image of RHS-4g RH
(e) SAED Pattern of RHS-1g RH

Table 1: Particle size analysis result of RHS from different masses of RH

Sample	Particle size (nm)
RHS-1g	69.988
RHS-4g	71.268

Figure 3 shows the EDS results of RHS from RH of varying masses under investigation in this research. The result indicates that the RHS-1gRH sample (Figure 3 (a))iscomposed mainly of Carbon (C), Oxygen (O), and silicon (Si) without any impurity while RHS-4g RH (Figure 3 (b)) is composed primarily of Carbon (C), Oxygen (O) and silicon (Si), albeit with minor impurities such asIr, Al and K that were not completely removed during acid pre-treatment.

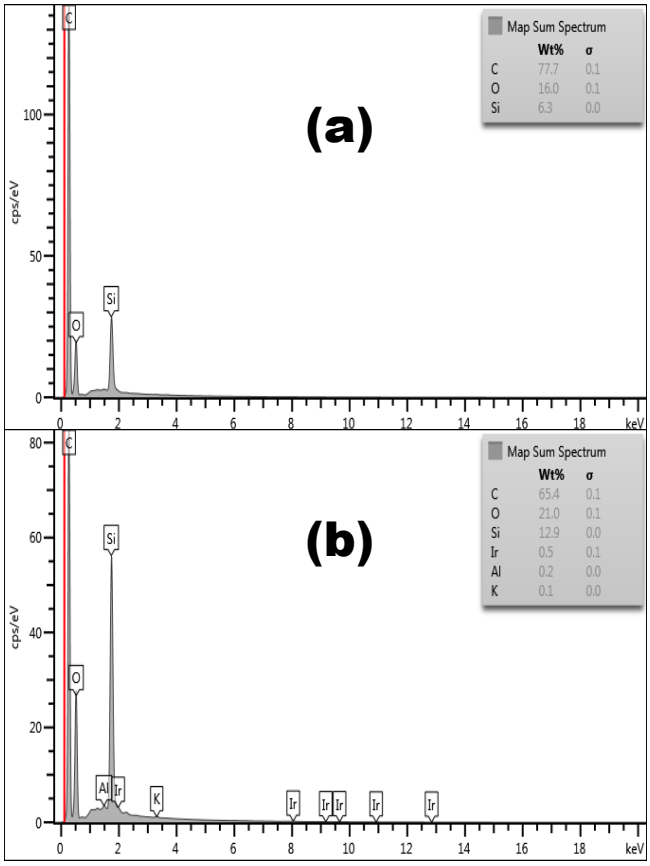


Fig 3. SEM-EDS of (a) RHS-1g RH (b) RHS-4g RH

3.3 UV-Vis Analysis (Diffuse Reflectance)

Figure 4 (a) showcases distinct diffuse reflectance spectra of RHS, derived from RH samples of varying masses (RHS-1g RH and RHS-4g RH). The absorption bands detected in RHS-1g RH are situated around 217, 249, 319, 474, and 519 nm, whereas in RHS-4g RH, they are at208, 249, and 319 nm. These absorption bands are attributed to defects or centers like oxygen deficiency centers[18] and carbon impurities (474 and 519 nm).

The Kubella-Munk and Tauc relations [19] have been used to determine the energy band gap of the samples. Figure 4 (b) demonstrates that the spectra of RHS-1g RH display three energy sets: 3.50 – 4.0, 4.0 – 5.30, and 5.3 0-5.78 eV. RHS-4g RH exhibits the same energy sets, except for 5.30 -5.78 eV, which ranges from 5.30 -6.21 eV. The energy bands peak at 3.90, 4.96, and 5.70 eV, respectively, for RHS-1g, and 3.90, 4.96, and 6.01 eV, respectively, for RHS-4g RH. These energy bands are a result of defects or centers in the silica. Both RHS-1g and RHS-4g have an equivalent band gap, which is approximately 5.29 eV.

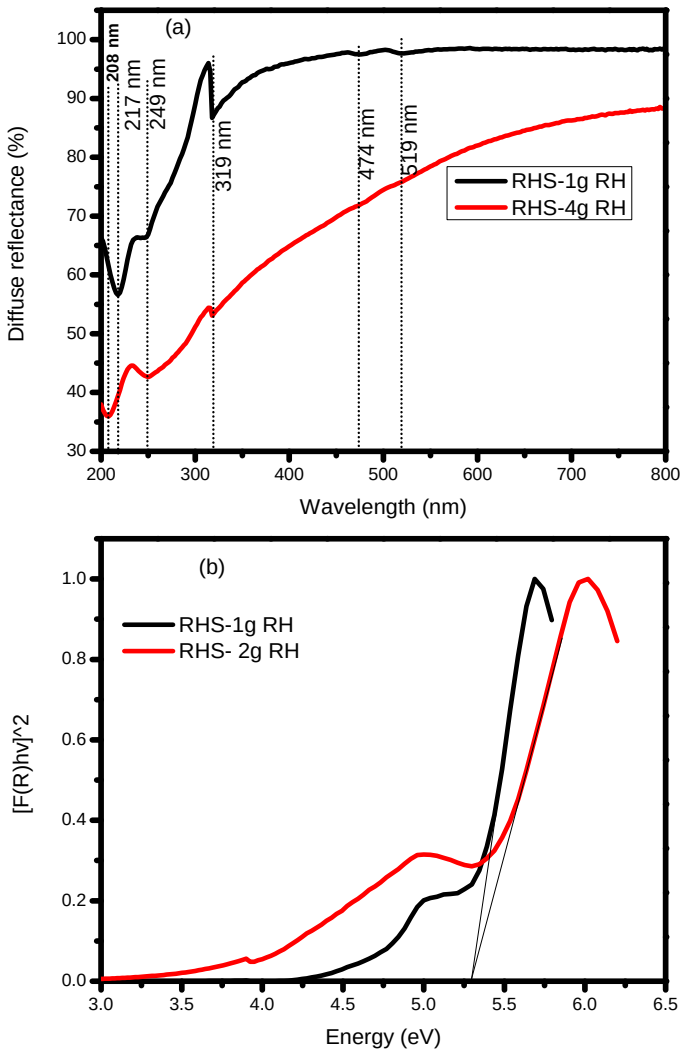


Fig 4. (a) Diffuse reflectance spectra (b) Band gap of RHS from RH of varying masses

3.4 Fourier Transform Infrared (FT-IR)

For the Fourier transform infrared (FT-IR) analysis of silica samples, we focused on one sample (RHS-5g). As can be seen in Figure 5 the absorption band that appears weak is in the range 700-867 cm^{-1}, with a valley at roughly 802 cm^{-1}, and can be attributed to symmetrical stretching vibrations of Si-O-Si [7,16,20,21]. On the other hand, the broadest band has a much stronger absorption between 867 cm-1 - 1300cm-1, with a valley at 1062 cm-1, which is due to the existence of carbon impurities [7] as supported by EDS. The formation of Si-O-C and C-O-C is responsible for the broadening and shift of the absorption wavenumber. Typically the vibrations linked to the broad and strong absorption band include the

asymmetrical stretching mode of Si-O-Si (1078 cm-1), Si-O-C (1100cm-1), and C-O-C (1260 cm-1) [7,15,20]. There are also weak bands with valleys at 1633 and 2341 cm-1 attributed to H-O-H bending mode and C=O bonds [21]in the carbon-incorporated silica, respectively. The absence of other strong peaks at 3000 cm-1 indicates that O-H stretching of the adsorbed H_2O molecules has been successfully removed during heat treatment[7,16]. Pure and relaxed silica with a bond angle of 144° has a narrow absorption band and valley at approximately 1078 cm-1 [13].The FT-IR analysis of rare earth ions doped nano-silica and undopedcarbon-incorporated silica derived from rice husk has been reported in various publications [13,14,22,23].

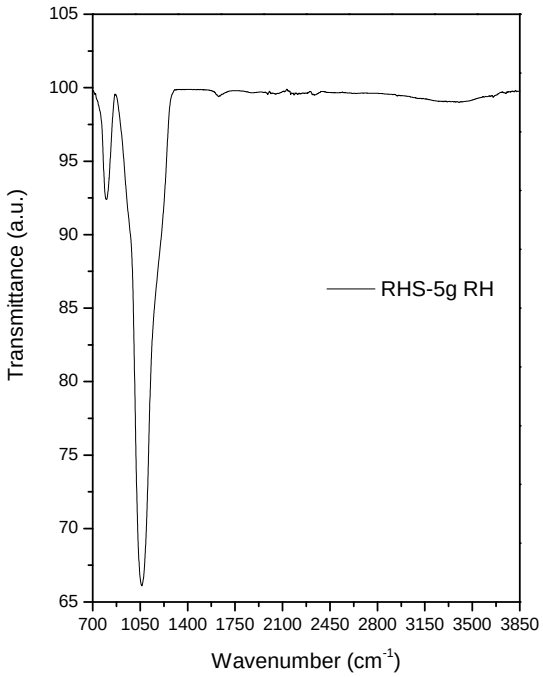


Fig 5. FT-IR spectrum of RHS – 5g RH

3.5 Brunauer-Emmett-Teller (BET) Analysis

A Brunauer-Emmett-Teller (BET) analysis was conducted on a SiO2 sample obtained from various varieties of RH (RHS-5g). The analysis revealed that this particular sample has a surface area of 291.42 m^2/g, a BJH pore volume of 0.33 cm^3/g, a pore size of 4.54 nm, and a BET constant (C) of 85.65. These results indicate that the sample is composed of mesoporous silica, which is consistent with findings from studies conducted by Liu et al. [9]and Wang et al. [2].

3.6 Photoluminescence analysis

In Figure 6 (a), the photoluminescence excitation (PLE) of various silica samples derived from RH of different masses (RHS-1g RH, RHS-2g RH, RHS-3g RH, RHS-4g RH, and RHS-5g RH) is displayed. The emission was monitored at 435 nm, and the resulting excitation spectra are broad and cover the range of 210-390 nm. Peaks are observed at approximately 215, 251, 275, and 365 nm. Figure 6 (b) shows the emission spectra of the same silica samples under the excitation wavelength of 365 nm, which is in the Near UV light region. The spectra are broad and continuous, covering the range of 380-650 nm. When excited at 215 nm in the far UV light region (Figure 6 (c)), the silica samples display discrete emission peaks at 415, 439, 452, 468, 485, 493, 525, 561, and 616 nm. These peaks indicate

emissions primarily in the blue (415, 439, 452, 468, 485, and 493 nm), green (525 and 561 nm), and red (616 nm) regions of the visible spectrum, resulting in white light with low intensity.

In Figure 7 (a), (b), and (c), the emissions under the excitation wavelength of 365 nm were deconvoluted using the spectrum of RHS-1g RH, RHS-3g RH, and RHS-5g RH, respectively. RHS-5g RH, which has a high amount of RH and probably high carbon residue, was deconvoluted into 6 peaks, with a maximum at about 403 nm (i), 414 nm (ii), 432 nm (iii), 453 nm (iv), 480 nm (v), and 519 nm (vi). RHS-1g RH and RHS-2g RH, which have low amounts of RH and probably low carbon residue, were deconvoluted into 5 separate peaks at about 412 nm (i), 435 nm (ii), 464 nm (iii), 490 nm (iv), and 522 nm (v). The emissions indicate that RHS primarily emits in the blue (403, 412-414, 432-435, 453-464, and 480-490 nm) and green (519-522 nm) regions of the visible spectrum. The peaks at 403, 412-414, 432-435, and 453-464 nm are due to defects or centers in the silica, such as oxygen-deficiency centers (ODCs) and non-bridging oxygen hole centers (NBOHC) [24–26] while the peaks at 480-490 and 519-522 nm are due to carbon impurities[2,7–9,24].

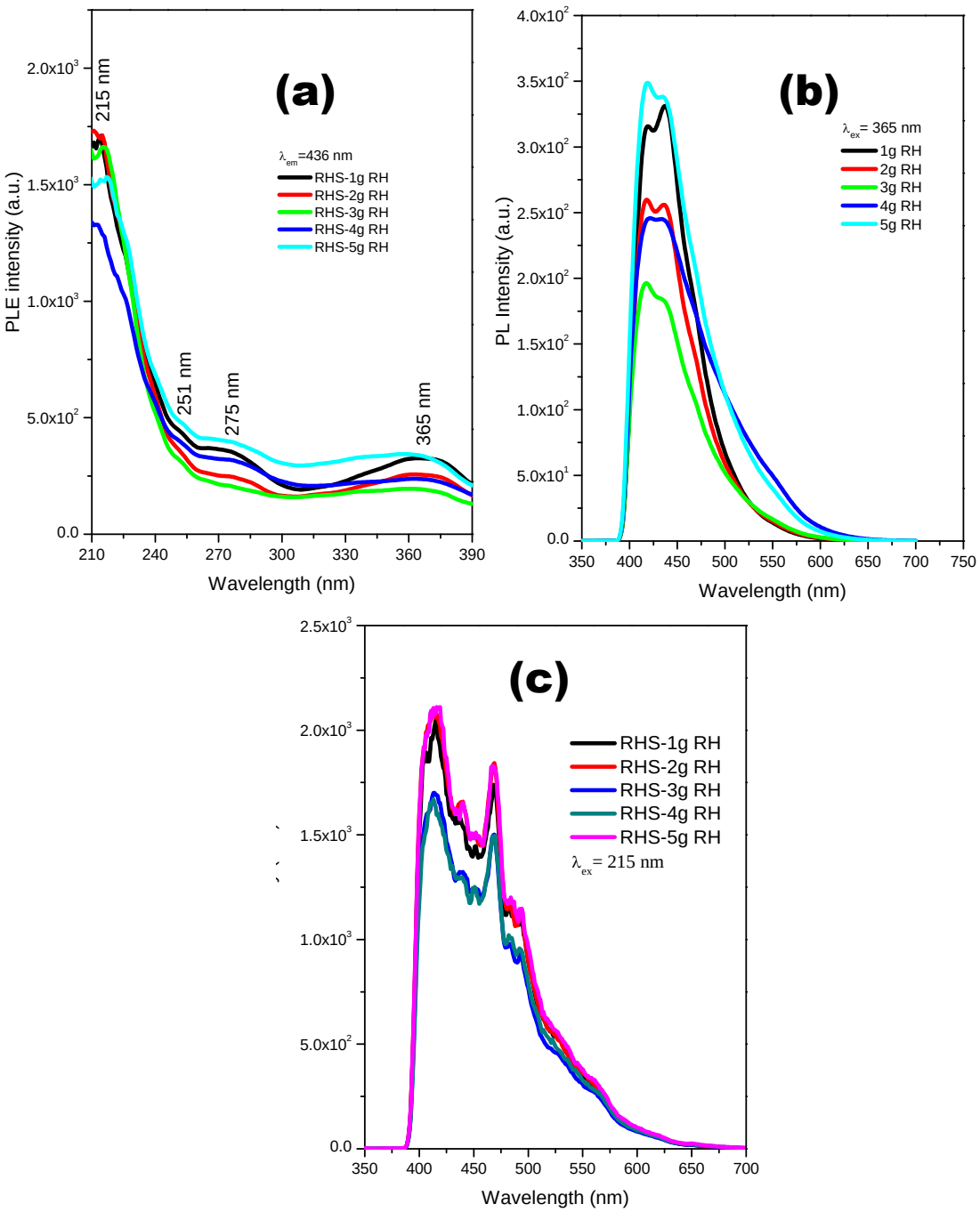


Fig 6. (a) Excitation (PLE) spectra (b) Emission (PL) spectra @ λ_{exc}=365 nm (c) Emission spectra @ λ_{exc}= 215 nm

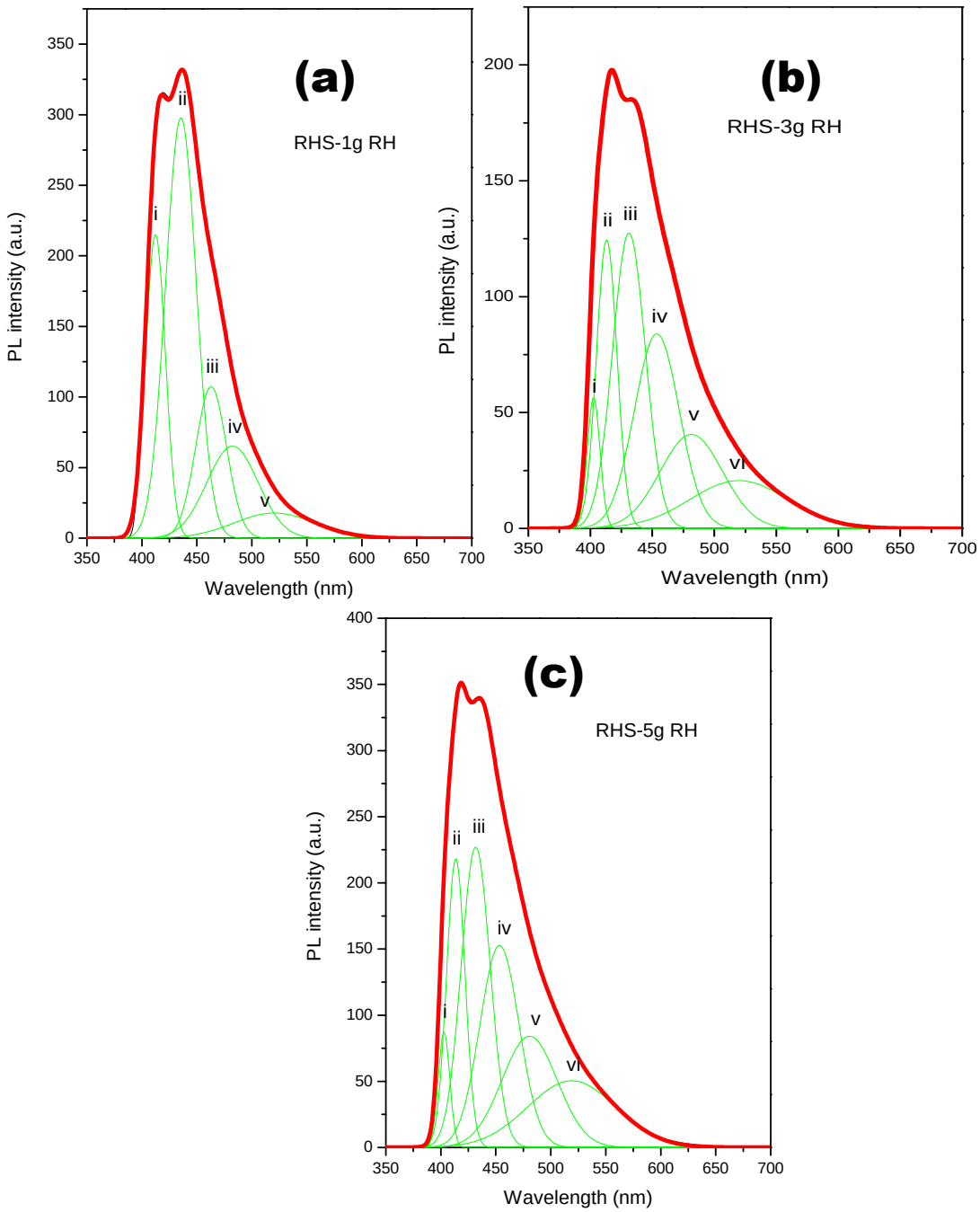


Fig 7. Deconvoluted Gaussian peaks of PL spectra of RHS derived from varying weights of rice (a) 1 g RH, (b) 3 g RH, and (c) 5 g RH

Figure 8 depicts the Commission Internationale de I'Eclairage (CIE) chromaticity diagram and coordinates respectively of emission spectra of silica samples derived from RH of different masses (RHS-1g RH, RHS-2g RH, RHS-3g RH, RHS-4g RH and RHS-5g RH), under 365 nm excitation. It shows emission in blue with CIE coordinates (0.155, 0.073), (0.157, 0.084), (0.160, 0.104), (0.160, 0.104), and (0.162, 0.120) for RHS-1g RH, RHS-2g RH, RHS-3g RH, RHS-4g RH, and RHS-5g RH respectively shown in Table 2.

The diagram in Figure 8 illustrates the Commission Internationale de I'Eclairage (CIE)chromaticity diagram. It also displays the coordinates of the emission spectra of silica samples that were obtained from different masses of RH (RHS-1g RH, RHS-2g RH, RHS-3g RH, RHS-4g RH, and RHS-5g RH) under 365 nm excitation. The emitted light is in the blue spectrum, with CIE coordinates of (0.155, 0.073), (0.157, 0.084), (0.160, 0.104), (0.160, 0.104), and (0.162, 0.120) respectively for RHS-1g RH, RHS-2g RH, RHS-3g RH, RHS-4g RH, and RHS-5g RH, as shown in Table 2.

Table 2 shows the color purity of RHS-x RH samples, where x ranges from 1 to 5g. As the amount of RH increases, the color purity decreases, resulting in a shift from blue to near-white light with 0% purity. This shift is caused by an increase in the carbon residue left in the samples, as explained by Chen in 2013.

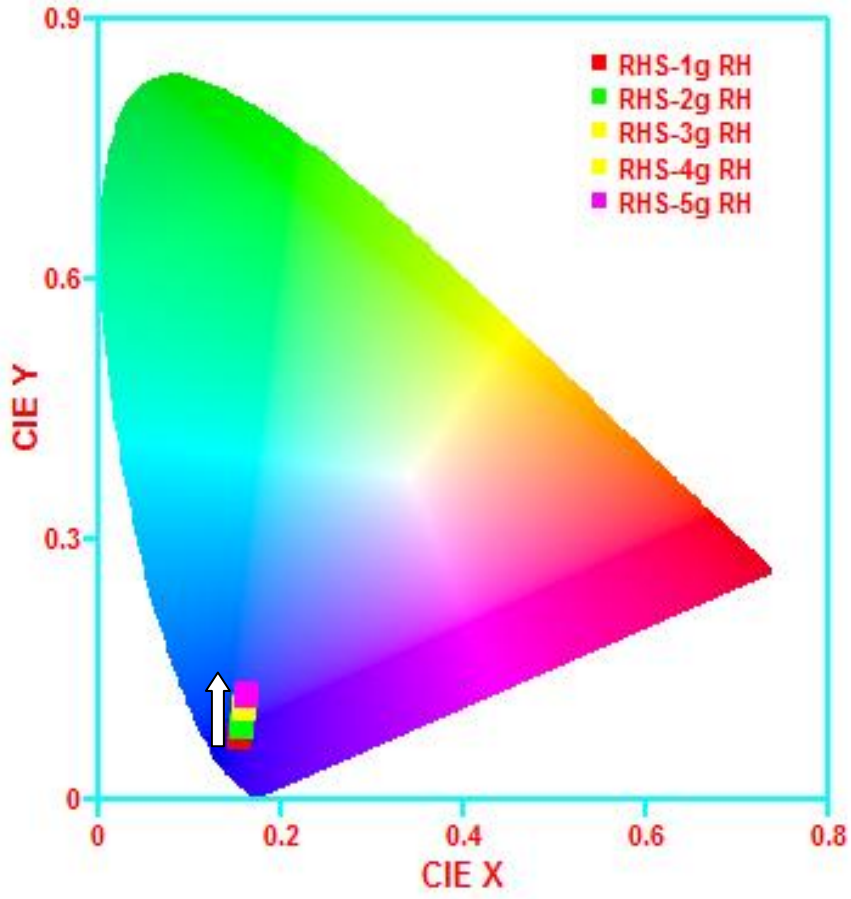


Fig 8. CIE chromaticity diagram of RHS samples from RHs of different masses.

Table 2: CIE chromaticity coordinates and color purity of RHS

RHS samples	x	y	Color purity (%)
RHS 1g RH	0.1547	0.0734	90.00
RHS 2g RH	0.1566	0.0844	87.14
RHS 3g RH	0.1596	0.1044	86.20
RHS 4g RH	0.1596	0.1044	86.20
RHS 5g RH	0.1619	0.1204	79.41

4.0 Conclusion

All the initial starting weights of rice husk considered for structural analysis produced nano-silicawhich is predominantly amorphous. The analysis of surface morphology revealed that all the samples containedclusters of spherical nanosized particles, with larger particles produced from higher starting weights of rice husk. The optical properties of the RHS are due to more than one defect or center, such as oxygen-deficiency centers (ODCs), non-bridging oxygen holecenters (NBOHC), and carbon impurities. The emission color of the RHS samples shifts from blue to near-white light as the weight of the starting RH increases due to an increase in the carbon residue left in the samples. Typically it is expected that the more the amount of starting RH the more the amount of carbon residue left after calcination. We could not determine the optimallevelof carbon residue for maximum fluorescence intensity due to the limited number of samples used in this research. However, we conclude by speculating that too much or too little carbon residue in RHS samples may negatively impact the fluorescence intensity and overall optical properties.

Funding. Tertiary Education Trust fund, Abuja, Nigeria.

Acknowledgment. This work was supported by the Tertiary Education Trust fund, in Abuja, Nigeria.

Disclosures. The author declares no conflict of interest.

Data availability. Data underlying the results presented in this paper are not publicly available at this time but may be obtained from the authors upon reasonable request.

REFERENCES

[1] W. Wang, J.C. Martin, N. Zhang, Harvesting silica nanoparticles from rice husks, J. Nanoparticle Res. 13 (2011) 6981–6990. https://doi.org/10.1007/s11051-011-0609-3.

[2] Z. Wang, S. Zeng, Y. Li, W. Wang, Z. Zhang, H. Zeng, W. Wang, L. Sun, Luminescence Mechanism of Carbon-Incorporated Silica Nanoparticles Derived from Rice Husk Biomass, Ind. Eng. Chem. Res. 56 (2017) 5906–5912. https://doi.org/10.1021/acs.iecr.7b00700.

[3] S.S. Nobre, X. Cattoën, R.A.S. Ferreira, M.W.C. Man, L.D. Carlos, Efficient spectrally dynamic blue-to-green emission of bipyridine-based bridged silsesquioxanes for solid-state lighting, Phys. Status Solidi - Rapid Res. Lett. 4 (2010) 55–57. https://doi.org/10.1002/pssr.200903396.

[4] M. Bardosova, M.E. Pemble, I.M. Povey, R.H. Tredgold, The langmuir-blodgett approach to making colloidal photonic crystals from silica spheres., Adv. Mater. 22 (2010) 3104–3124. https://doi.org/10.1002/adma.200903708.

[5] C.Z. and J. Lin, Chem Soc Rev and applications, (2012) 7938–7961. https://doi.org/10.1039/c2cs35215j.

[6] L.M. Rossi, L. Shi, F.H. Quina, Z. Rosenzweig, Stöber synthesis of monodispersed luminescent silica nanoparticles for bioanalytical assays, Langmuir. 21 (2005) 4277–4280. https://doi.org/10.1021/la0504098.

[7] Y. Ishikawa, S. Kawasaki, Y. Ishi, K. Sato, A. Matsumura, White photoluminescence from carbon-incorporated silica fabricated from rice husk, Jpn. J. Appl. Phys. 51 (2012). https://doi.org/10.1143/JJAP.51.01AK02.

[8] H. Chen, Biogenic silica nanoparticles derived from rice husk biomass and their applications, Texas State University, 2013.

[9] Y. Liu, Z. Wang, H. Zeng, C. Chen, J. Liu, L. Sun, W. Wang, Photoluminescent mesoporous carbon-doped silica from rice husks, Mater. Lett. 142 (2015) 280–282. https://doi.org/10.1016/j.matlet.2014.12.034.

[10] D.L. Green, J.S. Lin, Y.F. Lam, M.Z.C. Hu, D.W. Schaefer, M.T. Harris, Size, volume fraction, and nucleation of Stober silica nanoparticles, J. Colloid Interface Sci. 266 (2003) 346–358. https://doi.org/10.1016/S0021-9797(03)00610-6.

[11] M. Narisawa, T. Kawai, S. Watase, K. Matsukawa, T. Dohmaru, Long-Lived Photoluminescence in Amorphous Si – O – C(– H) Ceramics Derived from Polysiloxanes, 6 (2012) 1–6. https://doi.org/10.1111/j.1551-2916.2012.05425.x.

[12] R. Bryant, R. Proctor, A. Hawkridge, M. Jackson, A. Yeater, K. Counce, P. Yan, W. McClung, A. Fjellstrom, Genetic variation and association mapping of silica concentration in rice hulls using a germplasm collection, Genetica. 139 (2011) 1383–1398. https://doi.org/10.1007/s10709-012-9637-x.

[13] C. Mbakaan, I. Ahemen, F.B. Dejene, A.D. Onojah, S.J. Motloung, R. Ocaya, A. Reyes-Rojas, A. Reyes-Rojas, Structural and optical properties of nano-SiO_2 derived from the husk of some rice varieties and the effect of doping with Sm^{3+} ions, Opt. Mater. Express. 11 (2021) 965. https://doi.org/10.1364/OME.419552.

[14] C. Mbakaan, Effect of Some Physical Factors and Chemical Processing on the Yield and Quality of Nanosilica Derived from Rice Husk : Effectiveness of H3PO4 Pre-treatment on Structural and Optical Properties, Int. J. Eng. Appl. Phys. 3 (2023) 865–878.

[15] C. Lin, Y. Song, F. Gao, H. Zhang, Y. Sheng, K. Zheng, Z. Shi, X. Xu, H. Zou, Synthesis and luminescence properties of Eu(III)-doped silica nanorods based on the sol-gel process, J. Sol-Gel Sci. Technol. 69 (2014) 536–543. https://doi.org/10.1007/s10971-013-3254-8.

[16] L. Gong, H. Zou, G. Wang, Y. Sun, Q. Huo, X. Xu, Y. Sheng, Synthesis and luminescence properties of monodisperse SiO2@SiO2:Eu3+ microspheres, Opt. Mater. (Amst). 37 (2014) 583–588. https://doi.org/10.1016/j.optmat.2014.07.025.

[17] A.A. Mohsen, J.E. Mohammad, Electron Diffraction: in Modern Electron Microscopy in Physical and Life Sciences, in: Intechopen, 2016: p. 13. https://www.intechopen.com/books/advanced-biometric-technologies/liveness-detection-in-biometrics.

[18] M. Cannas, Point Defects in Amorphous SiO2: Optical Activity in the Visible, UV and Vacuum-UV Spectral Regions, Thesis. (1998) 1–151. http://scholar.google.com/scholar?hl=en&btnG=Search&q=intitle:Point+Defects+in+Amorphous+SiO+2+:+Optical+Activity+in+the+Visible,+UV+and+Vacuum-UV+Spectral+Regions#0%5Cnhttp://dsfa.fisica.unipa.it/~cannas/PhDThesis.PDF.

[19] S.N. Ogugua, H.C. Swart, O.M. Ntwaeaborwa, White light emitting LaGdSiO5:Dy3+nanophosphors for solid state lighting applications, Phys. B Condens. Matter. 480 (2016) 131–136. https://doi.org/10.1016/j.physb.2015.10.006.

[20] S. Duhan, P. Aghamkar, B. Lal, Influence of temperature and time on Nd-doped silica powder prepared by the solgel process, J. Alloys Compd. 474 (2009) 301–305.

https://doi.org/10.1016/j.jallcom.2008.06.095.
[21] Rachna Ahlawat, Synthesis and Characterizations of Europium doped Silica Nanophosphor., Int. J. Adv. Res. Sci. Eng. 6 (2017) 1077–1085.
[22] C. Mbakaan, I. Ahemen, A.N. Amah, A.D. Onojah, L. Koao, White-light-emitting Dy^{3+}-doped amorphous SiO<inf>2</inf> nanophosphors derived from rice husk, Appl. Phys. A Mater. Sci. Process. (2018). https://doi.org/10.1007/s00339-018-2156-6.
[23] C. Mbakaan, I. Ahemen, A.D. Onojah, A.N. Amah, K.G. Tshabalala, F.B. Dejene, Luminescent properties of Eu 3 + -doped silica nanophosphors derived from rice husk, Opt. Mater. (Amst). 108 (2020) 110168. https://doi.org/10.1016/j.optmat.2020.110168.
[24] A.E. Abbass, H.C. Swart, R.E. Kroon, White luminescence from sol–gel silica doped with silver, J. Sol-Gel Sci. Technol. 76 (2015) 708–714. https://doi.org/10.1007/s10971-015-3825-y.
[25] L.F. Koao, H.C. Swart, R.I. Obed, F.B. Dejene, Synthesis and characterization of Ce3 doped silica (SiO 2) nanoparticles, J. Lumin. 131 (2011) 1249–1254. https://doi.org/10.1016/j.jlumin.2010.10.038.
[26] R. Salh, Defect Related Luminescence in Silicon Dioxide Network : A Review, in: Cryst. Silicon - Prop. Uses, InTech, 2011: pp. 135–172.